

Feed-forward control for quantum state protection against decoherence

Chao-Quan Wang¹, Bao-Ming Xu¹, Jian Zou^{1,*}, Zhi He², Yan Yan¹, Jun-Gang Li¹, and Bin Shao¹

¹*School of Physics, Beijing Institute of Technology, Beijing 100081, China*

²*College of Physics and Electronics, Hunan University of Arts and Science, Changde 415000, China*

(Dated: January 23, 2021)

We propose a novel scheme of feed-forward control and its reversal for protecting quantum state against decoherence. Before the noise channel our pre-weak measurement and feed-forward are just to change the protected state into the state almost immune to the noise channel, and after the channel our reversed operations and post-weak measurements are just to restore the protected state. Unlike most previous state protection schemes, ours only concerns the noise channel and does not care about the protected state. We show that our scheme can effectively protect unknown states, nonorthogonal states and entangled states against amplitude damping noise. Our scheme has dramatic merits of protecting quantum states against heavy amplitude damping noise, and can perfectly protect some specific nonorthogonal states in an almost deterministic way, which might be found some applications in current quantum communication technology. And it is most important that our scheme is experimentally available with current technology.

PACS numbers: 03.67.Pp, 03.65.Ta, 02.30.Yy

I. INTRODUCTION

The dynamics of open quantum systems have been extensively studied. One of the major tasks is how to avoid the effect of decoherence due to interactions between system and its environment. To reduce the effect of decoherence, a large number of strategies have been proposed including decoherence-free subspaces [1–3], quantum error correction code [4–6], dynamical decoupling [7–9], quantum feedback control [10–15] etc. Controlling the dynamics of quantum system is the central goal in many areas of quantum physics. Recent experimental advances have enabled individual system to be monitored and manipulated at quantum level in real time [16–20], which makes quantum control more and more practical and realizable. Among different quantum control schemes, quantum feedback control is widely studied to improve the stability and robustness of the system, which is based on feeding back the measurement results to alter the future dynamics of quantum systems. The general framework of quantum feedback control was introduced by Wiseman and Milburn [10, 11], leading to relevant experimental achievements [21–23]. But information gain and disturbance in quantum systems are always antagonistic in quantum theory, and it is argued that a better feedback control scheme should reach a trade-off between them. Recently the proposed scheme of weak measurement-based feedback control has focused on achieving a balance for battling decoherence by setting proper measurement strength [24–26].

Recently there is a new trend in exploiting unknown quantum states to implement an advanced quantum communication and distributed quantum computation. For instance, quantum communication of an unknown state

from a photon to a photon and a blind quantum computation have been demonstrated experimentally [27, 28]. So how to protect an unknown quantum state against decoherence is of great significance. Most of previous works on quantum state protection using quantum measurement and feedback control have focused on protocols for known states [29], and few of them has addressed the issue of protecting unknown quantum states. It was suggested in Ref. [30] that there might not be any effective feedback control scheme to protect an unknown state and it was argued that because we do not know any information about the state of the system before the measurement, so after measurement we just obtain parts of information about the state, and then do not know how to do exactly. However, in Ref. [31] the authors have presented a scheme for protecting an unknown state of a qubit by weak measurement and measurement reversal.

It is well known that all existing quantum cryptosystems use nonorthogonal states as the carriers of information. Nonorthogonal states cannot be cloned (duplicated) by an eavesdropper. As a result, any eavesdropping attempt must introduce errors in the transmission, and it can be detected by the legal users of the communication channel. For example, two nonorthogonal states are used to encode information in the well-known B92 quantum key distribution protocol [32]. But the serious decoherence of commercial optical fibers which are widely used in quantum communication greatly limits the transmission distance. There is no doubt that protecting nonorthogonal states has great practical significance. Recently, feedback control schemes with weak measurement have been suggested for protecting nonorthogonal states [25, 26, 30, 33]. In Ref. [25], a qubit prepared in one of two nonorthogonal states and subsequently subjected to dephasing noise was discussed, and it was found that a quantum control scheme based on weak measurement with an appropriate measurement strength could realize the optimal recovery from the noise. However,

*Electronic address: zoujian@bit.edu.cn

these weak measurement-based feedback control schemes strongly depend on the nonorthogonal states to be protected, and the protecting effect is poor.

Now we reconsider feedback control with weak measurement from a new point of view and propose a novel scheme of feed-forward and its reversal against decoherence. It is noted that in previous schemes the intention for measurement is to acquire information of the protected states of system, and the feedback controls are applied to recover the state to the initial state based on the measurement result. In this paper, we exploit another effect of the measurement and feedback, i.e., they can transform any initial state into any given target state [30]. The procedure of our scheme is like this: Before the noise channel a pre-weak measurement is made and according to different measurement results an operation is applied in order to transform the protected state to some state (such as the states almost immune to the noise channel) and after the noise channel one can restore the state to the initial state with the reversed operations and weak measurement. Such a procedure is an example of feedback, which in this case is referred to as feed-forward, because the result of the operation implemented based on the result of the pre-weak measurement before the noise channel affects the dynamical behaviors of the system in the noise channel. In detail, our aim for pre-weak measurement and feed-forward is to intentionally drive the qubit close to its ground state before the noise channel, which can be thought of as a partial wave function collapse, and to restore the state to the initial state after the noise channel. Our scheme is universal for all initial states, i.e., all the initial states can be well protected by our scheme, but the protecting effect, i.e., the fidelity, is different and state-dependent. This means that we do not pay attention to the protected state in the whole process, and only concerns the noise channel in contrast to other schemes. Our scheme is consisted of weak and complete measurement before noise channel (pre-weak measurement) and reversed weak and incomplete (partial) measurements which select measurement result after noise channel (post-weak measurement) respectively. Meanwhile, according to different pre-weak measurement results, we add different feed-forward operation and its reversal into our scheme.

By using our scheme, we show that an unknown state, two nonorthogonal states and entangled state of two qubits can all be well protected probabilistically. For an arbitrary unknown state $|\psi_0\rangle = \alpha|0\rangle + \beta|1\rangle$, the protecting effect of our scheme is better than the scheme with weak measurement and measurement reversal in Ref. [31]. For instance, for all the quantum states with $|\beta| \geq |\alpha|$ and heavy amplitude damping noise, which are easier to cause the decoherence, our scheme can possess obviously superiority over that of Ref. [31]. Particularly, for protecting two nonorthogonal states, we can find some nonorthogonal states which can be perfectly protected in an almost deterministic way, while in Ref. [25], the scheme with a weak measurement followed by a feedback

control depends much on the initial nonorthogonal states, and the effect of protection is poor. At last, compared with Ref. [34] in which the weak measurement and measurement reversal have been used for protecting entangled state of two qubits, our scheme can achieve higher success probability for preserving the same amount of entanglement and particularly our scheme can completely circumvent entanglement sudden death (ESD) from decoherence.

The paper is structured as follows. In the next section, we introduce our scheme of weak-measurement-based feed-forward control. In Sec. III, we show how to use our scheme to protect an unknown state. In Sec. IV, we show how to use our scheme to protect two nonorthogonal states. In Sec. V, we show how to use our scheme to protect an entangled state of two qubits. In Sec. VI, we discuss the experimental feasibility of our scheme. At last, conclusion and discussion are given in Sec. VII.

II. WEAK-MEASUREMENT-BASED FEED-FORWARD CONTROL SCHEME

Now we introduce our weak-measurement-based feed-forward control scheme. In this paper, we only consider amplitude damping noise (AD) channel, which can be described as:

$$E_1 = \begin{pmatrix} 1 & 0 \\ 0 & \sqrt{1-r} \end{pmatrix}, E_2 = \begin{pmatrix} 0 & \sqrt{r} \\ 0 & 0 \end{pmatrix}, \quad (1)$$

where r is the magnitude of decoherence. Consider a qubit initially prepared in any state ρ , the decoherence effect of the channel can be represented as

$$\rho_\varepsilon = \sum_{i=1}^2 E_i \rho E_i^\dagger. \quad (2)$$

Our scheme of protecting a quantum state is consisted of one complete pre-weak measurement, two incomplete post-weak measurements and two feed-forward operations and their reversals, which is illustrated in Fig. 1. Before the noise channel the pre-weak measurement is chosen as $\Pi_1 = M_1^+ M_1$ and $\Pi_2 = M_2^+ M_2$, and M_1 and M_2 are represented respectively as

$$M_1 = \begin{pmatrix} \sqrt{p} & 0 \\ 0 & \sqrt{1-p} \end{pmatrix}, M_2 = \begin{pmatrix} \sqrt{1-p} & 0 \\ 0 & \sqrt{p} \end{pmatrix}, \quad (3)$$

where the pre-weak measurement is a complete measurement, i.e., $I = \sum_{i=1}^2 M_i^+ M_i$ and p is the pre-weak measurement strength.

The scheme for protecting quantum state is demonstrated as follows. For any initial state, first we make the pre-weak measurement. If result 1 (corresponding to $\Pi_1 = M_1^+ M_1$) is acquired, we choose a feed-forward operation before the noise channel, do-nothing F_1 , i.e.,

$$F_1 = \begin{pmatrix} 1 & 0 \\ 0 & 1 \end{pmatrix}, \quad (4)$$

and then let the qubit enter the decoherence channel. Consequently, after the noise channel a reversed operation we choose again is do-nothing F_1 . At last, we measure the qubit using partial weak measurement namely post-weak measurement $\Lambda = N_1^+ N_1$, and N_1 is represented as

$$N_1 = \begin{pmatrix} \sqrt{1-p_u} & 0 \\ 0 & 1 \end{pmatrix}, \quad (5)$$

where the post-weak measurement is weak and incomplete and p_u is the post-weak measurement strength.

If result 2 (corresponding to $\Pi_2 = M_2^+ M_2$) of the pre-weak measurement is acquired, we choose feed-forward operation F_2 as σ_x , i.e.,

$$F_2 = \begin{pmatrix} 0 & 1 \\ 1 & 0 \end{pmatrix}, \quad (6)$$

and then let the qubit enter the decoherence channel. Consequently, after the noise channel the reversed operation we choose again is operation F_2 , and it is noted that $F_2^2 = I$. At last, we measure the qubit using post-weak measurement $\Xi = W_1^+ W_1$, and W_1 is defined as

$$W_1 = \begin{pmatrix} 1 & 0 \\ 0 & \sqrt{1-p_v} \end{pmatrix}, \quad (7)$$

where the post-weak measurement is also weak and incomplete and p_v is the post-weak measurement strength. It is noted that the pre-weak measurement rather than projected measurement is necessary for our scheme because in this case the information about the initial quantum state can be preserved. And the post-weak measurement N_1 (W_1) is also very important, which is approximately the reversal of the corresponding pre-weak measurement M_1 (M_2), i.e., $M_1 N_1 \sim I$ and $M_2 W_1 \sim I$, and only in this way the information about the initial state can be retrieved. And after all these operations the original quantum state can be recovered. For clarity, we emphasize that in this paper we will frequently use these defined operators of measurements and feed-forward operations in the following sections.

III. PROTECTING UNKNOWN QUANTUM STATES

We first consider using our scheme to protect an arbitrary unknown quantum state. We assume that the qubit is initially prepared in an arbitrary state that we want to protect from the noise,

$$|\psi_0\rangle = \alpha|0\rangle + \beta|1\rangle. \quad (8)$$

First we measure $|\psi_0\rangle$ by using pre-weak measurement $\{M_1, M_2\}$. Depending on different measurement results, we classify the protecting process into two cases.

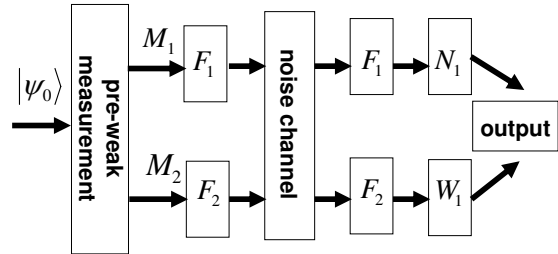


FIG. 1: A schematic diagram showing the procedure of our feed-forward control scheme for protecting an initial state. A qubit initially prepared in an arbitrary state $|\psi_0\rangle$, and before the noise channel a complete pre-weak measurement $\{M_1, M_2\}$ is made. If result 1 (corresponding to M_1) is acquired, a feed-forward operation do-nothing F_1 is applied. And the qubit is allowed to enter the noise channel and after the noise channel a reversed operation also do-nothing F_1 is applied, and then a post-weak incomplete measurement N_1 is made. If result 2 (corresponding to M_2) is acquired, a feed-forward operation F_2 is applied. And the qubit is allowed to enter the noise channel and after the noise channel a reversed operation also F_2 is applied, and then a post-weak incomplete measurement W_1 is made. At last the output state, which is close to the initial state, is obtained.

Case one: If result 1 is acquired, the qubit state becomes

$$|\psi_0^{m1}\rangle = \frac{M_1|\psi_0\rangle}{\sqrt{\langle\psi_0|\Pi_1|\psi_0\rangle}} \quad (9)$$

with the probability $g^{m1} = \langle\psi_0|\Pi_1|\psi_0\rangle = |\alpha|^2 p + |\beta|^2 (1-p)$. Then we adopt the feed-forward operation of do-nothing

$$\begin{aligned} |\psi_0^{f1}\rangle &= F_1|\psi_0^{m1}\rangle = \alpha^{f1}|0\rangle + \beta^{f1}|1\rangle \\ &= \frac{1}{\sqrt{g^{m1}}}(\alpha\sqrt{p}|0\rangle + \beta\sqrt{1-p}|1\rangle). \end{aligned} \quad (10)$$

After a period of τ in the decoherence channel, the qubit state is no longer pure because of energy relaxation with the rate Γ . However, it is technically easier to use the mathematical trick of unraveling the relaxation into “jump” and “no jump” scenarios and work with pure states [31]. Through the decoherence channel of the amplitude damping, the qubit trajectories can be viewed as two parts including “jumping” into the state $|0\rangle$ with the “jump” probability $g^{j1} = g^{m1}|\beta^{f1}|^2(1 - e^{-\Gamma\tau})$ and the evolution, i.e., “no jumping” into the state

$$|\psi_0^{e1}\rangle = \frac{1}{\sqrt{g^{e1}}}(\alpha\sqrt{p}|0\rangle + \beta\sqrt{1-p}e^{-\Gamma\frac{\tau}{2}}|1\rangle) \quad (11)$$

with the “no jump” probability $g^{e1} = |\alpha|^2 p + |\beta|^2 (1-p)e^{-\Gamma\tau}$. Then the reversed operation we adopt is still do-nothing. The qubit state from the “no jumping” trajectory becomes

$$|\psi_0^{u1}\rangle = F_1|\psi_0^{e1}\rangle = |\psi_0^{e1}\rangle, \quad (12)$$

and the qubit state from the “jumping” trajectory becomes

$$|\psi_0^{ju1}\rangle = F_1|0\rangle = |0\rangle. \quad (13)$$

At last we measure the qubit by using the post-weak measurement $\Lambda = N_1^\dagger N_1$ and obtain the measured state from the “no jumping” trajectory

$$\begin{aligned} |\psi_0^{n1}\rangle &= \frac{N_1|\psi_0^{u1}\rangle}{\sqrt{\langle\psi_0^{u1}|\Lambda|\psi_0^{u1}\rangle}} \\ &= \frac{1}{\sqrt{g^{n1}}}(\alpha\sqrt{p}\sqrt{1-p_u}|0\rangle + \beta\sqrt{1-pe^{-\Gamma\frac{\tau}{2}}}|1\rangle) \end{aligned} \quad (14)$$

with the probability $g^{n1} = |\alpha|^2 p(1-p_u) + |\beta|^2 (1-p)e^{-\Gamma\tau}$. The state $|\psi_0^{ju1}\rangle$ from the “jumping” trajectory becomes $|0\rangle$ with the probability $g^{jn1} = g^{j1}(1-p_u) = g^{m1}|\beta f^1|^2(1-e^{-\Gamma\tau})(1-p_u)$. The density matrix description of the final qubit state can be written as

$$\rho_0^{fin1} = \frac{g^{n1}|\psi_0^{n1}\rangle\langle\psi_0^{n1}| + g^{jn1}|0\rangle\langle 0|}{g^{n1} + g^{jn1}} \quad (15)$$

with the success (selection) probability and fidelity respectively

$$g^{fin1} = g^{n1} + g^{jn1}, \quad (16)$$

$$f^{fin1} = \langle\psi_0|\rho_0^{fin1}|\psi_0\rangle. \quad (17)$$

Case two: If we obtain result 2 in the pre-weak measurement, the qubit state becomes

$$|\psi_0^{m2}\rangle = \frac{M_2|\psi_0\rangle}{\sqrt{\langle\psi_0|\Pi_2|\psi_0\rangle}} \quad (18)$$

with the probability $g^{m2} = \langle\psi_0|\Pi_2|\psi_0\rangle = |\alpha|^2(1-p) + |\beta|^2 p$, and we adopt the feed-forward operation of F_2

$$\begin{aligned} |\psi_0^{f2}\rangle &= F_2|\psi_0^{m2}\rangle = \alpha f^2|0\rangle + \beta f^2|1\rangle \\ &= \frac{1}{\sqrt{g^{m2}}}(\beta\sqrt{p}|0\rangle + \alpha\sqrt{1-p}|1\rangle). \end{aligned} \quad (19)$$

Then like case one, we let the qubit go through the decoherence channel and we also view the qubit trajectories as two parts “jumping” into the state $|0\rangle$ with the “jump” probability $g^{j2} = g^{m2}|\beta f^2|^2(1-e^{-\Gamma\tau})$ and the evolution, i.e., “no jumping” into the state

$$|\psi_0^{e2}\rangle = \frac{1}{\sqrt{g^{e2}}}(\beta\sqrt{p}|0\rangle + \alpha\sqrt{1-pe^{-\Gamma\frac{\tau}{2}}}|1\rangle) \quad (20)$$

with the probability $g^{e2} = |\beta|^2 p + |\alpha|^2(1-p)e^{-\Gamma\tau}$. After the noise channel the reversed operation we apply is still

F_2 , and the qubit state of the “no jumping” trajectory becomes

$$\begin{aligned} |\psi_0^{u2}\rangle &= F_2|\psi_0^{e2}\rangle \\ &= \frac{1}{\sqrt{g^{e2}}}(\alpha\sqrt{1-pe^{-\Gamma\frac{\tau}{2}}}|0\rangle + \beta\sqrt{p}|1\rangle), \end{aligned} \quad (21)$$

and the qubit state of the “jumping” trajectory becomes

$$|\psi_0^{ju2}\rangle = F_2|0\rangle = |1\rangle. \quad (22)$$

At last we measure the qubit by using the post-weak measurement $\Xi = W_1^\dagger W_1$ and obtain the following state from the “no jumping” trajectory

$$\begin{aligned} |\psi_0^{w1}\rangle &= \frac{W_1|\psi_0^{u2}\rangle}{\sqrt{\langle\psi_0^{u2}|\Xi|\psi_0^{u2}\rangle}} \\ &= \frac{1}{\sqrt{g^{w1}}}(\alpha\sqrt{1-pe^{-\Gamma\frac{\tau}{2}}}|0\rangle + \beta\sqrt{p}\sqrt{1-p_v}|1\rangle) \end{aligned} \quad (23)$$

with the probability $g^{w1} = |\alpha|^2(1-p)e^{-\Gamma\tau} + |\beta|^2 p(1-p_v)$. The state $|\psi_0^{ju2}\rangle$ from the “jumping” trajectory becomes $|1\rangle$ with the probability $g^{jw1} = g^{j2}(1-p_v) = g^{m2}|\beta f^2|^2(1-e^{-\Gamma\tau})(1-p_v)$. The density matrix description of the final qubit state can be written as

$$\rho_0^{fin2} = \frac{g^{w1}|\psi_0^{w1}\rangle\langle\psi_0^{w1}| + g^{jw1}|1\rangle\langle 1|}{g^{w1} + g^{jw1}} \quad (24)$$

with the success (selection) probability and fidelity respectively

$$g^{fin2} = g^{w1} + g^{jw1}, \quad (25)$$

$$f^{fin2} = \langle\psi_0|\rho_0^{fin2}|\psi_0\rangle. \quad (26)$$

After completing the whole measurement and feed-forward process, the final total success probability and the final total fidelity can be expressed respectively as

$$g^{fin} = g^{fin1} + g^{fin2}, \quad (27)$$

$$f^{fin} = \frac{g^{fin1}f^{fin1} + g^{fin2}f^{fin2}}{g^{fin}}. \quad (28)$$

It is noted that if we let $1 - e^{-\Gamma\tau} = r$, the decoherence channel described in this section is the same as the channel mentioned in section II.

A. Exact protection

It is noted that in case one if we take the post-weak measurement strength as

$$p_u = 1 - \frac{(1-p)e^{-\Gamma\tau}}{p} = 1 - \frac{(1-p)(1-r)}{p}, \quad (29)$$

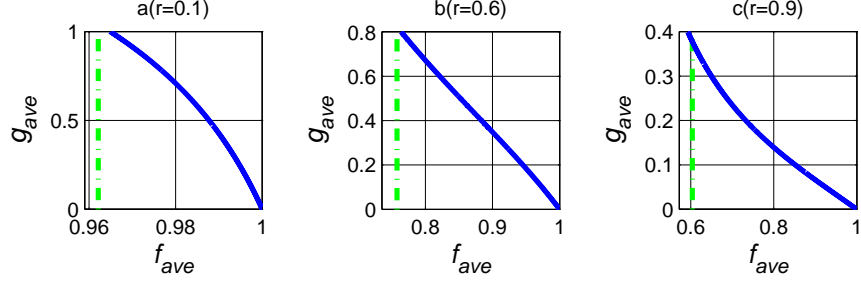


FIG. 2: (Color online). Under the exact protecting condition, f_{ave} - g_{ave} phase diagrams for a: $r=0.1$, b: $r=0.6$ and c: $r=0.9$. The green dotted lines represent the fidelity without any measurement and feed-forward.

the measured qubit state $|\psi_0^{n1}\rangle$ in Eq. (14) along the “no jumping” trajectory will be the initial state, i.e., $|\psi_0^{n1}\rangle = |\psi_0\rangle$, which would be an exact restoration of the initial state, and we define it as an exact protection. And analogously, in case two if we take the weak measurement strength

$$p_v = 1 - \frac{(1-p)e^{-\Gamma\tau}}{p} = 1 - \frac{(1-p)(1-r)}{p}, \quad (30)$$

the measured qubit state $|\psi_0^{w1}\rangle$ in Eq. (23) along the “no jumping” trajectory will be the initial state, i.e., $|\psi_0^{w1}\rangle = |\psi_0\rangle$, which would also be an exact restoration of the initial state. We define Eqs. (29) and (30) as an exact protecting condition in our scheme. It can be seen from Eqs. (29, 30) that because p_u and $p_v \geq 0$, $p \in [\frac{1-r}{2-r}, 1]$. Under this condition, for an arbitrary state, the final total success probability and the final total fidelity become respectively

$$\begin{aligned} g^{fin} &= g^{fin1} + g^{fin2} \\ &= \frac{(1-p)^2 r(1-r)}{p} + 2(1-p)(1-r), \end{aligned} \quad (31)$$

$$\begin{aligned} f^{fin} &= \frac{g^{fin1} f^{fin1} + g^{fin2} f^{fin2}}{g^{fin}} \\ &= \frac{\frac{2(1-p)^2 r(1-r)}{p} |\alpha|^2 |\beta|^2}{\frac{(1-p)^2 r(1-r)}{p} + 2(1-p)(1-r)} \\ &= \frac{2(1-p)(1-r)}{\frac{(1-p)^2 r(1-r)}{p} + 2(1-p)(1-r)}. \end{aligned} \quad (32)$$

It is noted that the average success probability is still g^{fin} due to its independence of the state, but for clarity, we still define a symbol g_{ave} ($= g^{fin}$) as the average success probability. From numerical calculation we find that the fidelity will increase with the measurement strength p , and when we choose p close to 1, the fidelity will approach 1, that means we can make the final qubit state arbitrarily close to the initial state under the exact protection. On the contrary, the success probability

We can see that in this case the final total success probability is independent of the state. However, the final total fidelity is state dependent. An arbitrary state on the Bloch sphere can be represented in terms of $\alpha = \cos \frac{\theta}{2}$ and $\beta = e^{i\phi} \sin \frac{\theta}{2}$. If we take an average over the whole Bloch sphere, we obtain the average fidelity f_{ave}

$$\begin{aligned} f_{ave} &= \frac{1}{4\pi} \int_0^{2\pi} \int_0^\pi f^{fin} \sin \theta d\theta d\phi \\ &= \frac{\frac{(1-p)^2 r(1-r)}{3p} + 2(1-p)(1-r)}{\frac{(1-p)^2 r(1-r)}{p} + 2(1-p)(1-r)}. \end{aligned} \quad (33)$$

will decrease with the measurement strength p , when we choose p close to 1, the success probability almost drops to 0.

Under the exact protecting condition, the relation between the average fidelity f_{ave} and the average success probability g_{ave} is shown in Fig. 2. As an example, we only show the protecting effect of an unknown state for $r = 0.1, 0.6$ and 0.9 . It can be seen that our scheme greatly improves the fidelity than that without any mea-

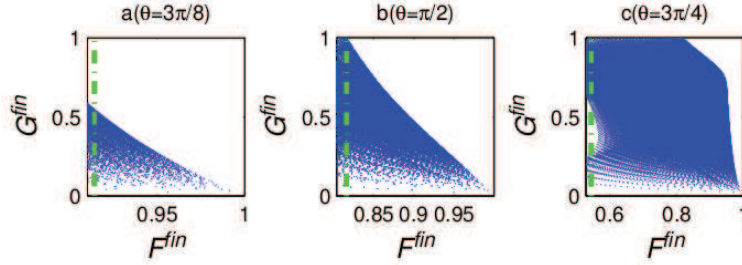


FIG. 3: (Color online). F^{fin} - G^{fin} phase diagrams for protecting some given states a: $\theta = \frac{3\pi}{8}$, b: $\theta = \frac{\pi}{2}$ and c: $\theta = \frac{3\pi}{4}$. We set $r = 0.6$ and $\phi = 0$ for three diagrams. The optimal protection is given by the boundary lines of the blue region. The green dotted lines represent the fidelity without any measurement and feed-forward.

surement and feed-forward. Especially, our scheme can protect an arbitrary unknown state even for heavy amplitude damping noise (e.g., $r=0.9$).

B. Optimal protection

In part A, we discuss the exact protection of an arbitrary unknown state, which demands p_u and p_v having specific relationship with p . However, this kind of protection is not an optimal protection. Actually all mea-

surement strength p, p_u and p_v can be varied independently from 0 to 1 so that by varying them we can obtain the highest success probability (fidelity) for fixed fidelity (success probability) for an arbitrary unknown state. We call this kind of protection as optimal protection and the corresponding groups of measurement strength p, p_u and p_v as optimal protecting condition. Now we show the optimal protection of an unknown state by using our scheme. According to Eqs. (27) and (28), for an arbitrary state, the final total success probability and the final total fidelity can be expressed respectively as

$$\begin{aligned}
 G^{fin} &= G^{fin1} + G^{fin2} \\
 &= p(1-p_u)|\alpha|^2 + (1-p)(1-p_u)r|\beta|^2 + p(1-p_v)|\beta|^2 \\
 &\quad + (1-p)(1-p_v)r|\alpha|^2 + (1-p)(1-r),
 \end{aligned} \tag{34}$$

$$\begin{aligned}
 F^{fin} &= \frac{G^{fin1}F^{fin1} + G^{fin2}F^{fin2}}{G^{fin}} \\
 &= \frac{p(1-p_u)|\alpha|^4 + (1-p)(1-r)|\beta|^4 + (1-p)(1-p_u)r|\alpha|^2|\beta|^2 + 2\sqrt{p}\sqrt{1-p}\sqrt{1-p_u}\sqrt{1-r}|\alpha|^2|\beta|^2}{p(1-p_u)|\alpha|^2 + (1-p)(1-p_u)r|\beta|^2 + p(1-p_v)|\beta|^2 + (1-p)(1-p_v)r|\alpha|^2 + (1-p)(1-r)} + \\
 &\quad \frac{(1-p)(1-r)|\alpha|^4 + p(1-p_v)|\beta|^4 + (1-p)(1-p_v)r|\alpha|^2|\beta|^2 + 2\sqrt{p}\sqrt{1-p}\sqrt{1-p_v}\sqrt{1-r}|\alpha|^2|\beta|^2}{p(1-p_u)|\alpha|^2 + (1-p)(1-p_u)r|\beta|^2 + p(1-p_v)|\beta|^2 + (1-p)(1-p_v)r|\alpha|^2 + (1-p)(1-r)}.
 \end{aligned} \tag{35}$$

An arbitrary state on the Bloch sphere can be represented in terms of $\alpha = \cos\frac{\theta}{2}$ and $\beta = e^{i\phi}\sin\frac{\theta}{2}$. For an arbitrary state, it is clear that each group of measurement strength (p, p_u, p_v) uniquely determines its corresponding fidelity and success probability denoted by one point (F^{fin}, G^{fin}) . When the measurement strengths p, p_u, p_v

are independently taken over all the real numbers from 0 to 1, we obtain F^{fin} (the fidelity)- G^{fin} (success probability) phase diagram. We first show the protecting effect of several states with $\theta = \frac{3\pi}{8}, \frac{\pi}{2}, \frac{3\pi}{4}$ and $\phi = 0$ for $r = 0.6$ in Fig. 3.

It is noted that for given fidelity (succuss probability), the point (F^{fin}, G^{fin}) , at which the succuss probability

(fidelity) is maximized, is distributed on the boundary of the phase diagram. All the points distributed on the

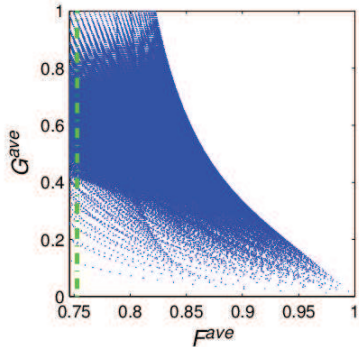


FIG. 4: (Color online). F^{ave} - G^{ave} phase diagram. The green dotted line represents the fidelity without any measurement and feed-forward.

boundary line of the phase diagram correspond to the optimal protection and we denote these special points by the optimal fidelity F_{opt}^{fin} and the optimal success probability G_{opt}^{fin} . These groups of measurement strength (p, p_u, p_v) corresponding to the optimal protection points $(F_{opt}^{fin}, G_{opt}^{fin})$ on the boundary line are optimal groups of measurement strength (i.e., optimal protecting condition). The boundary line of the phase diagram indicates the relationship between the fidelity and the success probability under optimal protecting condition. From Fig. 3 we can see that under the optimal protecting condition, the larger $|\beta|/|\alpha|$ becomes, the more superiority our scheme has, which is very important in quantum communication due to these states being much easier to be influenced by the noise channel. In Ref. [29] the optimal quantum feedback control based on weak measurement is available for all typical types of noise sources, but the approach is valid only for some suitable quantum states and the fidelity has only an improvement less than three percent compared with that without any measurement and feedback. Compared with Ref. [29], our scheme can probabilistically protect an arbitrary state with higher fidelity.

IV. PROTECTING TWO NONORTHOGONAL STATES

In previous section, we show how to use our scheme to protect an unknown quantum state, and in this section we will show that it is more effective to protect two known nonorthogonal states. It is noted that the procedure of protecting each one of two nonorthogonal states is the same as that of protecting an arbitrary state mentioned in section III. Consider two nonorthogonal states that we

Now we consider optimal protection of an unknown state. By taking average over the whole Bloch sphere, the average success probability G^{ave} and the average fidelity F^{ave} can be expressed respectively as

$$G^{ave} = \frac{1}{4\pi} \int_0^{2\pi} \int_0^\pi G^{fin} \sin\theta d\theta d\phi. \quad (36)$$

$$F^{ave} = \frac{1}{4\pi} \int_0^{2\pi} \int_0^\pi F^{fin} \sin\theta d\theta d\phi. \quad (37)$$

For $r = 0.6$, we plot F^{ave} - G^{ave} phase diagram in Fig. 4. Similarly we can obtain the optimal protection and corresponding condition in this case. The average optimal protection points $(F_{opt}^{ave}, G_{opt}^{ave})$ with the average fidelity F_{opt}^{ave} and the average success probability G_{opt}^{ave} under the optimal protecting condition lie on the boundary of the phase diagram. It can be seen from Fig. 4 that the average fidelity can be much larger than that without measurement and feed-forward (green dotted line), even close to 1. Of course, it is at the cost of the decrease of the success probability. However, compared with the scheme of Ref. [31] based on weak measurement and measurement reversal without feed-forward control, our scheme can reach higher success probability for fixed fidelity. In addition, we find that our scheme is obviously superior over that of Ref. [31] at any degree of amplitude damping, and the heavier the amplitude damping noise, the better protecting effect of our scheme than that of their scheme. As an example, under the optimal protecting condition, we numerically compare our scheme (boundary lines of the blue region) with that in Ref. [31] (boundary lines of the red region) for $r = 0.1, 0.6$ and 0.9 in Fig. 5. We can see that under the optimal protection, our scheme is always better than that in Ref. [31]. In particular, when the amplitude damping is large such as $r = 0.9$, our scheme has an obvious advantage. The feature of our scheme has practical significance in current communication, due to larger decoherence in commercial optical fibers with long transmission distance.

want to protect from noise,

$$\begin{aligned} |\psi_{\pm}\rangle &= \cos\frac{\theta}{2}|+\rangle \pm e^{i\phi} \sin\frac{\theta}{2}|-\rangle \\ &= \frac{1}{\sqrt{2}}(\cos\frac{\theta}{2} \pm e^{i\phi} \sin\frac{\theta}{2})|0\rangle + \\ &\quad \frac{1}{\sqrt{2}}(\cos\frac{\theta}{2} \mp e^{i\phi} \sin\frac{\theta}{2})|1\rangle \\ &= \alpha_{\pm}|0\rangle + \beta_{\pm}|1\rangle, \end{aligned} \quad (38)$$

where $|\pm\rangle = \frac{1}{\sqrt{2}}(|0\rangle \pm |1\rangle)$, $\alpha_{\pm} = \frac{1}{\sqrt{2}}(\cos\frac{\theta}{2} \pm e^{i\phi} \sin\frac{\theta}{2})$ and $\beta_{\pm} = \frac{1}{\sqrt{2}}(\cos\frac{\theta}{2} \mp e^{i\phi} \sin\frac{\theta}{2})$. It is noted that the

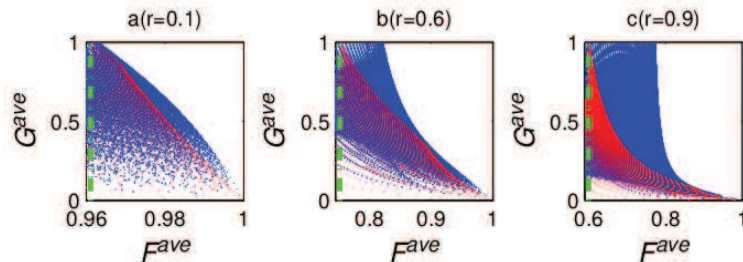


FIG. 5: (Color online). F^{ave} - G^{ave} phase diagrams for different amplitude damping a: $r=0.1$, b: $r=0.6$ and c: $r=0.9$. The blue region is corresponding to the results of our scheme, and the red region is corresponding to that of Ref. [31]. The green dotted lines represent the fidelity without any measurement and feed-forward.

nonorthogonal states $|\psi_{\pm}\rangle$ are more general than that in Refs. [25, 26]. The overlapping of the two nonorthogonal states can be quantified by

$$\langle\psi_{+}|\psi_{-}\rangle = \cos\theta, \quad (39)$$

which is independent of ϕ . The range of θ and ϕ is respectively from 0 to $\frac{\pi}{2}$ and from 0 to 2π .

A. Exact protection

Under the exact protecting condition $p_u = 1 - \frac{(1-p)(1-r)}{p}$ and $p_v = 1 - \frac{(1-p)(1-r)}{p}$, the final total success probability and the final total fidelity of each one of two nonorthogonal states can be obtained from Eqs. (31) and (32)

$$g_{\pm}^{fin} = \frac{(1-p)^2 r(1-r)}{p} + 2(1-p)(1-r), \quad (40)$$

$$f_{\pm}^{fin} = \frac{\frac{2(1-p)^2 r(1-r)}{p} |\alpha_{\pm}|^2 |\beta_{\pm}|^2}{\frac{(1-p)^2 r(1-r)}{p} + 2(1-p)(1-r)} + \frac{2(1-p)(1-r)}{\frac{(1-p)^2 r(1-r)}{p} + 2(1-p)(1-r)}. \quad (41)$$

Substituting $\alpha_{\pm} = \frac{1}{\sqrt{2}}(\cos\frac{\theta}{2} \pm e^{i\phi} \sin\frac{\theta}{2})$ and $\beta_{\pm} = \frac{1}{\sqrt{2}}(\cos\frac{\theta}{2} \mp e^{i\phi} \sin\frac{\theta}{2})$ into Eq. (41), we obtain

$$f_{\pm}^{fin} = \frac{\frac{(1-p)^2 r(1-r)}{2p} |\cos\frac{\theta}{2} \pm e^{i\phi} \sin\frac{\theta}{2}|^2 |\cos\frac{\theta}{2} \mp e^{i\phi} \sin\frac{\theta}{2}|^2}{\frac{(1-p)^2 r(1-r)}{p} + 2(1-p)(1-r)} + \frac{2(1-p)(1-r)}{\frac{(1-p)^2 r(1-r)}{p} + 2(1-p)(1-r)}. \quad (42)$$

It can be seen from Eqs. (40) and (42) that the success probability and the fidelity are the same for both $|\psi_{\pm}\rangle$. Particularly, the success probability does not depend on the nonorthogonal states. And for each one of the two nonorthogonal states, as p increases, the fidelity increases, and on the contrary the success probability decreases. As an example we give the protecting effect for different pairs of nonorthogonal states ($|\psi_{+}\rangle, |\psi_{-}\rangle$) with $(\theta, \phi) = (\frac{3\pi}{8}, \frac{\pi}{16}), (\frac{\pi}{4}, \frac{9\pi}{8}), (\frac{\pi}{8}, \frac{7\pi}{4})$ for $r = 0.6$ in Fig. 6. The trade-off relation between the success probability and the fidelity is clearly shown in Fig. 6. Although, the protecting effect for different nonorthogonal states are slightly different, it is obvious that the application of our scheme increases the fidelity comparing with that

without any measurement and feed-forward scheme. It should be emphasized that our scheme can effectively protect any pair of two nonorthogonal states, i.e., for any θ and ϕ on the Bloch sphere under the exact protecting condition.

B. Optimal protection

In part A, we discuss the exact protection of two nonorthogonal states, and in this part, we show optimal protection of two nonorthogonal states. It is noted that the average optimal protection of two nonorthogonal

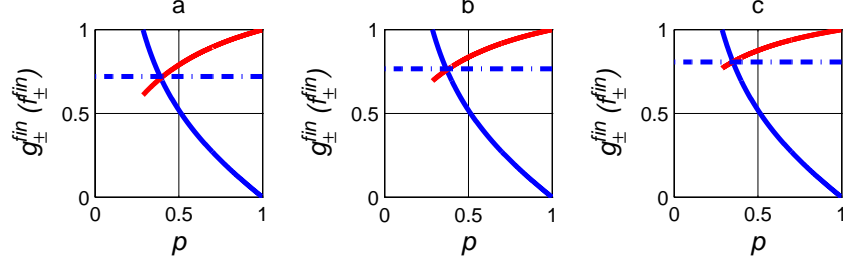


FIG. 6: (Color online). Under the exact protecting condition, the effect of protecting two nonorthogonal states for a: $\theta = \frac{3\pi}{8}, \phi = \frac{\pi}{16}$; b: $\theta = \frac{\pi}{4}, \phi = \frac{9\pi}{8}$; c: $\theta = \frac{\pi}{8}, \phi = \frac{7\pi}{4}$ and $r = 0.6$. The blue (red) solid lines represent the relationship between the success probability (the fidelity) and measurement strength p . The blue dotted lines represent the fidelity without any measurement and feed-forward.

states is very similar to the average optimal protection of an unknown state. According to Eqs. (34) and (35), we can obtain the success probability and the fidelity

for each one of two nonorthogonal states, which can be expressed respectively as

$$G_{\pm}^{fin} = G_{\pm}^{fin1} + G_{\pm}^{fin2} \\ = p(1-p_u)|\alpha_{\pm}|^2 + (1-p)(1-p_u)r|\beta_{\pm}|^2 + p(1-p_v)|\beta_{\pm}|^2 + (1-p)(1-p_v)r|\alpha_{\pm}|^2 + (1-p)(1-r), \quad (43)$$

$$F_{\pm}^{fin} = \frac{G_{\pm}^{fin1}F_{\pm}^{fin1} + G_{\pm}^{fin2}F_{\pm}^{fin2}}{G_{\pm}^{fin}} \\ = \frac{p(1-p_u)|\alpha_{\pm}|^4 + (1-p)(1-r)|\beta_{\pm}|^4 + (1-p)(1-p_u)r|\alpha_{\pm}|^2|\beta_{\pm}|^2 + 2\sqrt{p}\sqrt{1-p}\sqrt{1-p_u}\sqrt{1-r}|\alpha_{\pm}|^2|\beta_{\pm}|^2}{p(1-p_u)|\alpha_{\pm}|^2 + (1-p)(1-p_u)r|\beta_{\pm}|^2 + p(1-p_v)|\beta_{\pm}|^2 + (1-p)(1-p_v)r|\alpha_{\pm}|^2 + (1-p)(1-r)} + \\ \frac{(1-p)(1-r)|\alpha_{\pm}|^4 + p(1-p_v)|\beta_{\pm}|^4 + (1-p)(1-p_v)r|\alpha_{\pm}|^2|\beta_{\pm}|^2 + 2\sqrt{p}\sqrt{1-p}\sqrt{1-p_v}\sqrt{1-r}|\alpha_{\pm}|^2|\beta_{\pm}|^2}{p(1-p_u)|\alpha_{\pm}|^2 + (1-p)(1-p_u)r|\beta_{\pm}|^2 + p(1-p_v)|\beta_{\pm}|^2 + (1-p)(1-p_v)r|\alpha_{\pm}|^2 + (1-p)(1-r)}. \quad (44)$$

Now we assume that the probability of two nonorthogonal states to be generated is equal. The success probability and fidelity for two nonorthogonal states can be written respectively as

$$G_{non}^{fin} = \frac{G_{+}^{fin} + G_{-}^{fin}}{2} \\ = p(1-p_u) + p(1-p_v) + (1-p)(1-p_u)r \\ + (1-p)(1-p_v)r + 2(1-p)(1-r), \quad (45)$$

$$F_{non}^{fin} = \frac{F_{+}^{fin} + F_{-}^{fin}}{2}. \quad (46)$$

We can see that our scheme can well protect two nonorthogonal states under the optimal protecting con-

dition. For two given nonorthogonal states, i.e., for given θ and ϕ , we can plot $F_{non}^{fin}-G_{non}^{fin}$ phase diagram. Similarly we can obtain the optimal protection and the corresponding condition in this case. The optimal protection points $(F_{non}^{opt}, G_{non}^{opt})$ with the fidelity F_{non}^{opt} and the success probability G_{non}^{opt} under the optimal protecting condition lie on the boundary of the phase diagram. As an example, we numerically demonstrate the optimal protection of different nonorthogonal states for $r = 0.6$ in Fig. 7.

Especially when $\theta = \frac{7\pi}{16}, \phi = 0$, the fidelity and

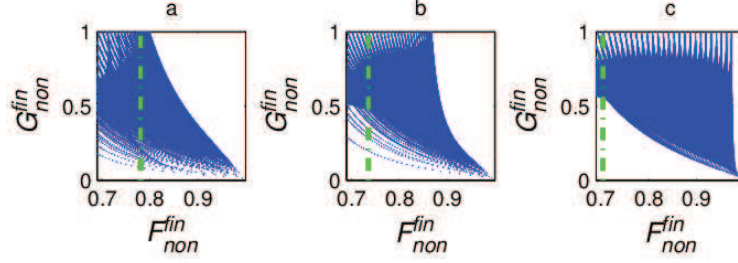


FIG. 7: (Color online). F_{non}^{fin} - G_{non}^{fin} phase diagrams of protecting two nonorthogonal states a: $\theta = \frac{3\pi}{16}, \phi = 0$; b: $\theta = \frac{5\pi}{16}, \phi = 0$; c: $\theta = \frac{7\pi}{16}, \phi = 0$ with $r = 0.6$. The green dotted lines represent the fidelity without any measurement and feed-forward control.

the success probability can respectively reach 0.98 and 0.9949 as shown in Fig. 7(c) and the corresponding optimal group of measurement strength is $p = 0.995$, $p_u = 0.0052$ and $p_v = 0.005$. Compared with Ref. [25], the protecting effect of our scheme for two nonorthogonal states is much better. The scheme in Ref. [25] depends much on the initial nonorthogonal states and is not effective, while our scheme can effectively protect any pair of nonorthogonal states.

V. PROTECTING ENTANGLED STATE

It is noted that our scheme can also protect multipartite quantum state. Now we consider a two-qubit (labeled by a and b) quantum system whose initial state is $|\Phi\rangle = \alpha|00\rangle + \beta|11\rangle$. We assume that the two qubits being in different environments go respectively through two independent quantum channels with damping rates r_a and r_b . By using our scheme for each of the two qubits, we can protect this entangled state of the two qubits. According to the pre-weak measurement results for each qubit, we can classify our protecting scheme into four cases, i.e., $M_{c1} = M_1^a \otimes M_1^b$, $M_{c2} = M_2^a \otimes M_2^b$, $M_{c3} = M_1^a \otimes M_2^b$ and $M_{c4} = M_2^a \otimes M_1^b$, where

$$M_1^i = \begin{pmatrix} \sqrt{p^i} & 0 \\ 0 & \sqrt{1-p^i} \end{pmatrix}, M_2^i = \begin{pmatrix} \sqrt{1-p^i} & 0 \\ 0 & \sqrt{p^i} \end{pmatrix}, (i = a, b).$$

It is noted that the pre-weak measurement of two qubits is complete, i.e., $I = \sum_{i=1}^4 M_{ci} M_{ci}^\dagger$. We define the feed-forward operations as

$$F_1^a = F_1^b = \begin{pmatrix} 1 & 0 \\ 0 & 1 \end{pmatrix}, F_2^a = F_2^b = \begin{pmatrix} 0 & 1 \\ 1 & 0 \end{pmatrix}, \quad (47)$$

and the post-weak measurements as

$$N_1^i = \begin{pmatrix} \sqrt{1-p_u^i} & 0 \\ 0 & 1 \end{pmatrix}, W_1^i = \begin{pmatrix} 1 & 0 \\ 0 & \sqrt{1-p_v^i} \end{pmatrix}, (i = a, b). \quad (48)$$

Case one: If result 1 (M_{c1}) is acquired, the feed-forward operation and its reversed operation are both

chosen as $F_1^a \otimes F_1^b$ and the post-weak measurement is chosen as $N_1^a \otimes N_1^b$.

Case two: If result 2 (M_{c2}) is acquired, the feed-forward operation and its reversed operation are both chosen as $F_2^a \otimes F_2^b$ and the post-weak measurement is chosen as $W_1^a \otimes W_1^b$.

Case three: If result 3 (M_{c3}) is acquired, the feed-forward operation and its reversed operation are both chosen as $F_1^a \otimes F_2^b$ and the post-weak measurement is chosen as $N_1^a \otimes W_1^b$.

Case four: If result 4 (M_{c4}) is acquired, the feed-forward operation and its reversed operation are both chosen as $F_2^a \otimes F_1^b$ and the post-weak measurement is chosen as $W_1^a \otimes N_1^b$.

In each case, the final density matrix can be written as

$$\rho^i = \frac{1}{P_i} \begin{pmatrix} \rho_{11}^i & 0 & 0 & \rho_{14}^i \\ 0 & \rho_{22}^i & 0 & 0 \\ 0 & 0 & \rho_{33}^i & 0 \\ \rho_{41}^i & 0 & 0 & \rho_{44}^i \end{pmatrix} \quad (49)$$

with the success probability $P_i = \rho_{11}^i + \rho_{22}^i + \rho_{33}^i + \rho_{44}^i$. All the elements of the density matrixes can be analytically obtained, but for brevity we do not give them in this paper. And the concurrence can be written as

$$C_i = \max\{0, \Omega_i \equiv \frac{2(|\rho_{14}^i| - \sqrt{\rho_{22}^i \rho_{33}^i})}{P_i}\}, (i = 1, 2, 3, 4). \quad (50)$$

The final success probability of our whole scheme is

$$P_{fin} = P_1 + P_2 + P_3 + P_4, \quad (51)$$

and the final concurrence is

$$C_{fin} = \frac{P_1 C_1 + P_2 C_2 + P_3 C_3 + P_4 C_4}{P_{fin}}. \quad (52)$$

It is noted that we can still discuss the exact protection and the optimal protection of the entangled state, but for simplicity we only consider the exact protection. In

this paper, we consider the identical decoherence channel $r_a = r_b = 0.6$ and the identical pre-weak measurement strength $p^a = p^b$ for both qubits under the exact protection, that is $p_u^a = p_v^a = 1 - \frac{(1-p^a)(1-r_a)}{p^a}$ and $p_u^b = p_v^b = 1 - \frac{(1-p^b)(1-r_b)}{p^b}$. It is obvious that each value of $p^a (= p^b)$ uniquely determines a success probability and corresponding concurrence. When we take p^i over all the real numbers from $\frac{1-r_i}{2-r_i}$ to 1, ($i = a, b$), we obtain P_{fin} (the success probability)- C_{fin} (concurrence) phase diagram. It was shown in Ref. [34] that a scheme based on weak measurement and measurement reversal can also protect an entangled state of two qubits under its exact protecting condition. As an example, we compare our result with that of Ref. [34] in Fig. 8, and for convenience we choose the same entangled state used in Ref. [34], i.e., $|\alpha\rangle = 0.42$. From Fig. 8 one can see that the success probability of our scheme is much higher than that in Ref. [34] for the same amount of entanglement, that means the protecting effect of our scheme is much better than that in Ref. [34]. And the concurrence from our scheme could be approximatively kept at a value of 0.15 with success probability close to 1.

The ESD condition without measurement and feed-forward control is $\sqrt{r_a r_b} \geq \frac{|\alpha|}{|\beta|}$ for the initial state Φ with $|\beta| \geq |\alpha|$ and the ESD condition of the scheme in Ref. [34] is $(1-p^a)(1-p^b) \geq \frac{1}{r_a r_b} \left| \frac{\alpha}{\beta} \right|^2$. But in our scheme the ESD never appears. As decoherence increases, the complete ESD without measurement and feed-forward must occur, and in Ref. [34] the success probability of preserving some amount of entanglement is approaching zero. However, our scheme still can preserve part of entanglement with considerable success probability, in another word, at any degree of decoherence, the ESD never appears for our scheme, which is very different from that of Ref. [34]. As an example, we plot the success probability and the entanglement phase diagram for $|\alpha| = 0.42$, $r_a = r_b = 0.9$ and $p^a = p^b$, and compare our results with that of Ref. [34] in Fig. 9. From Fig. 9 one can see that when the concurrence is less than 0.2, our scheme can obtain a considerable success probability and as the concurrence drops down to 0, the success probability of our scheme will be close to 1, which means that the ESD will never appear in our scheme, but for the scheme of Ref. [34], when the concurrence is 0, the success probability is also approaching 0, i.e., the complete ESD occurs in this case.

VI. EXPERIMENTAL FEASIBILITY

It should be noted that our scheme can be realized experimentally with current technology. The experimental realization of the weak measurement before the noise channel was discussed theoretically in Ref. [35], and it was shown that this kind of weak measurement can be realized by coupling the system to a meter and performing the usual projective measurements on the meter only.

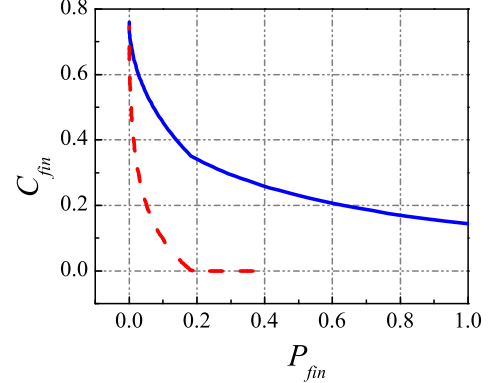


FIG. 8: (Color online). P_{fin} - C_{fin} phase diagram of the effect of protecting entangled state for $|\alpha| = 0.42$, $r_a = r_b = 0.6$ and $p^a = p^b$. The blue solid line represents our scheme and the red dashed line represents the scheme in Ref. [34]. It is noted that in this case the concurrence without any measurement and feed-forward is zero.

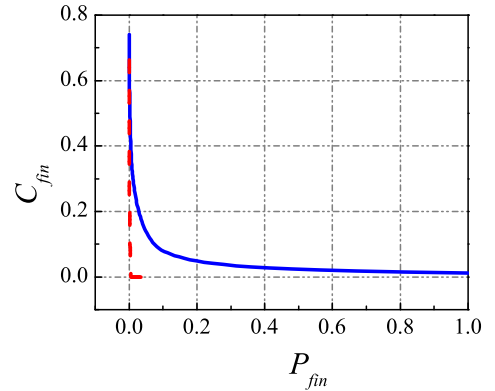


FIG. 9: (Color online). P_{fin} - C_{fin} phase diagram for $|\alpha| = 0.42$, $r_a = r_b = 0.9$ and $p^a = p^b$. The blue solid line represents our scheme and the red dashed line represents the scheme in Ref. [34]. It is noted that in this case the concurrence without any measurement and feed-forward is zero.

The experimental implementation was realized recently in a photonic architecture [26]. The required weak measurement on the signal qubit (photon) is realized by entangling it with another meter qubit (photon), and then a full-strength projective measurement is performed on the meter qubit, which implements a measurement on the signal qubit with a strength (ranging from 0 to 1) determined by the input meter state. The weak measurement after the noise channel has been demonstrated experimentally [34]. In Ref. [34], the weak measurement (corresponding to weak measurement $\Xi = W_1^+ W_1$ after the noise channel in our scheme) and the reversing measurement (corresponding to weak measurement $\Lambda = N_1^+ N_1$ after the noise channel in our scheme) for a single-photon polarization qubit are implemented with Brewster-angle

glass plates (BPs) and wave plates. As the BP probabilistically rejects vertical polarization ($|1\rangle_s$) and completely transmits horizontal polarization ($|0\rangle_s$), a single-photon polarization qubit found behind a BP had been subject to weak measurement or partial collapse measurement towards $|0\rangle_s$. The reversing measurement is designed to reverse the effect of weak measurement by making partial collapse measurement towards $|1\rangle_s$ and it can be implemented by adding 45° half-wave plates (HWPs) before and after the BPs. The weak measurement and the reversing measurement strengths can be varied by changing the number of BPs.

VII. CONCLUSION AND DISCUSSION

In this paper, we have proposed a novel scheme of feed-forward control for protecting quantum states against amplitude-damping noise. We have demonstrated that by using our scheme an unknown quantum state, two known nonorthogonal quantum states and two-qubit entangled state can be effectively protected. Especially, our scheme is more effective for protecting the vulnerable qubit states, i.e., the states in which the population in the excited level is higher than that in the ground level, and works well even for heavy amplitude damping. For some known nonorthogonal states, our scheme can achieve a perfect protection in an almost deterministic way. And for two-qubit entangled state our scheme can completely avoid the entanglement sudden death no matter how heavy the amplitude damping noise is.

Now we compare the effect of our scheme with other protecting schemes. In Ref. [25], a quantum feedback control scheme based on weak measurement was proposed to realize the optimal protection of two nonorthogonal states against dephasing noise. In Ref. [29], this method is extended to fighting against other types of noise sources. But this scheme is valid only for some suitable states and the fidelity has only an improvement less than three percent compared with that without any measurement and feedback. In contrast, our scheme can protect any quantum state and for some nonorthogonal states can realize almost perfect protection in an almost deterministic way. Actually our scheme is quite distinctive from that in Ref. [25, 29], the purpose of our measurement and feed-forward is totally different from that in Ref. [25, 29]. Before the noise channel our main purpose for choosing measurement and feed-forward operation is to make the initial state transformed into the state almost immune to the noise channel and after the channel our aim is to recover the state to the initial state. In the process, we do not care about the information about the quantum state being protected. But in their works, the objective to measure is to obtain information about the initial quantum state and then the corresponding feed-back operation is to turn the measured state into the initial state according to the knowledge extracted from the measurement. In other words, our choice of the mea-

surement and feed-forward only concerns the noise channel, while the measurement and feedback in Ref. [25, 29] mainly concerns the protected quantum state. On the other hand recently a scheme based on weak measurement and measurement reversal was proposed to protect an arbitrary qubit state [31] and a two-qubit entangled state [34]. In this paper we have shown that the success probability for fixed fidelity in Ref. [31] is lower than ours at any degree of amplitude damping, and our scheme has obvious superiority over the scheme in Ref. [31, 34] for heavy amplitude damping noise and for the vulnerable states which is easier to deteriorate in the noise channel. Compared with the result in Ref. [34] our scheme can achieve higher success probability for keeping the same amount of entanglement and completely avoid the ESD, while the success probability of preserving some amount of entanglement for their scheme is approaching zero for heavy damping noise. This can be understood as follows. In our scheme, the pre-measurement is complete and none of the pre-measurement results has been discarded. In addition, according to any one of the pre-measurement results, we can not only effectively reserve some information about the initial state which would be used to recover the initial state in the following steps, but also transform them into these states almost immune to the noise channel. This characteristics ensures that our scheme can obtain a higher success probability for given fidelity.

It should be pointed out that our scheme can be found applications in the B92 protocol which is the simplest quantum key distribution (QKD) protocol conceived by Bennett in 1992 [36]. The B92 protocol is based on only two nonorthogonal states associated with the two values of the logical bit to be secretly transmitted. Despite its simplicity, the B92 protocol is considered as a quite impractical protocol mainly for its low tolerance to noise of a communication channel. The high dependence on channel noise can be ascribed to the so-called unambiguous state discrimination) attack [37], which represents the principal threat against the B92 protocol, and severely limits its performances. But one might use our scheme to overcome this difficulty. Before sending the signal to Bob, Alice can use our pre-weak measurement and feed-forward to prepare the state to the state almost immune to the noise, and then Alice sends it to Bob through the fiber and tells Bob the pre-weak measurement results through classical communication, and when Bob receives the signal he can use our reversed operation and the reversed post-weak measurement to restore the information sent by Alice originally. It has been shown that our scheme can perfectly protect some kind of nonorthogonal states with almost certainty. In one word, our scheme is very significant for improving the efficiency and security of quantum communication due to the fact that the transmission distance is greatly limited by the serious decoherence of commercial optical fibers now widely used in quantum communication. It is worth noting that our scheme is entirely feasible with

current technology. In the end, we also hope that the idea of our feed-forward control scheme in this paper provides new thinking for fully utilization of quantum measurement-based control method in the future.

ACKNOWLEDGMENT

This work was supported by the National Natural Science Foundation of China (Grants Nos. 11274043, 11375025).

-
- [1] G. M. Palma, K. A. Suominen, and A. K. Ekert, *Proc. R. Soc. A* **452**, 567 (1996).
- [2] P. Zanardi, M. Rasetti, *Phys. Rev. Lett* **79**, 3306 (1997).
- [3] D. A. Lidar, I. L. Chuang, and K. B. Whaley, *Phys. Rev. Lett.* **81**, 2594 (1998).
- [4] A. R. Calderbank, and P. W. Shor, *Phys. Rev. A* **54**, 1098 (1996).
- [5] E. Knill, and R. Laflamme, *Phys. Rev. A* **55**, 900 (1997).
- [6] A. M. Steane, *Phys. Rev. Lett.* **77**, 793 (1996).
- [7] L. Viola, and S. Lloyd, *Phys. Rev. A* **58**, 2733 (1998).
- [8] P. Zanardi, *Phys. Lett. A* **258**, 77 (1999).
- [9] L. Viola, E. Knill, and S. Lloyd, *Phys. Rev. Lett.* **82**, 2417 (1999).
- [10] H. M. Wiseman, and G. J. Milburn, *Phys. Rev. Lett.* **70**, 548 (1993).
- [11] H. M. Wiseman, *Phys. Rev. A* **49**, 2133 (1994).
- [12] H. M. Wiseman, S. Mancini, and J. Wang, *Phys. Rev. A* **66**, 013807 (2002).
- [13] S. Mancini, *Phys. Rev. A* **73**, 010304 (R) (2006).
- [14] A. R. R. Carvalho, and J. J. Hope, *Phys. Rev. A* **76**, 010301(R) (2007).
- [15] A. R. R. Carvalho, A. J. S. Reid, and J. J. Hope, *Phys. Rev. A* **78**, 012334 (2008).
- [16] C. J. Hood, M. S. Chapman, T. W. Lynn, and H. J. Kimble, *Phys. Rev. Lett.* **80**, 4157 (1998).
- [17] B. Julsgard, A. Kozhekin, and E. S. Polzik, *Nature (London)* **413**, 400 (2001).
- [18] W. Lu, Z. Ji, L. Pfeiffer, K. W. West, and A. J. Rimberg, *Nature (London)* **423**, 422 (2003).
- [19] J. M. Geremia, J. K. Stockton, and H. Mabuchi, *Science* **304**, 270 (2004).
- [20] A. Öttl, S. Ritter, M. Köhl, and T. Esslinger, *Phys. Rev. Lett.* **95**, 090404 (2005).
- [21] W. P. Smith, J. E. Reiner, L. A. Orozco, S. Kuhr, and H. M. Wiseman, *Phys. Rev. Lett.* **89**, 133601 (2002).
- [22] M. A. Armen, J. K. Au, J. K. Stockton, A. C. Doherty, and H. Mabuchi, *Phys. Rev. Lett.* **89**, 133602 (2002).
- [23] M. D. Lahaye, O. Buu, B. Camarota, and K. C. Schwab, *Science* **304**, 74 (2004).
- [24] T. Pramanik, and A. S. Majumdar, *Phys. Lett. A* **377**, 3209 (2013).
- [25] A. M. Branczyk, P. E. M. F. Mendonca, A. Gilchrist, A. C. Doherty, and S. D. Bartlett, *Phys. Rev. A* **75**, 012329 (2007).
- [26] G. G. Gillett, R. B. Dalton, B. P. Lanyon, M. P. Almeida, M. Barbieri, G. J. Pryde, J. L. O'Brien, K. J. Resch, S. D. Bartlett, and A. G. White, *Phys. Rev. Lett.* **104**, 080503 (2010).
- [27] D. Boschi, S. Branca, F. De Martini, L. Hardy, and S. Popescu, *Phys. Rev. Lett.* **80**, 1121 (1998).
- [28] S. Barz, E. Kashefi, A. Broadbent, J. F. Fitzsimons, A. Zeilinger, and P. Walther, *Science* **335**, 303 (2012).
- [29] X. Xiao, and M. Feng, *Phys. Rev. A* **83**, 054301 (2011).
- [30] Y. Yan, J. Zou, B. M. Xu, J. G. Li, and B. Shao, *Phys. Rev. A* **88**, 032320 (2013).
- [31] A. N. Korotkov, and K. Keane, *Phys. Rev. A* **81**, 040103(R) (2010).
- [32] C. H. Bennett, *Science* **257**, 752 (1992).
- [33] Y. Yang, X. Y. Zhang, J. Ma, and X. X. Yi, *Phys. Rev. A* **87**, 012333 (2013).
- [34] Y. S. Kim, J. C. Lee, O. Kwon, and Y. H. Kim, *Nature Physics* **8**, 117 (2012).
- [35] J. Audretsch, T. Konrad, and A. Scherer, *Phys. Rev. A* **63**, 052102 (2001).
- [36] C. H. Bennett, *Phys. Rev. Lett.* **68**, 3121 (1992).
- [37] M. Dusek, N. Lütkenhaus, and M. Hendrich, *Prog. Opt.* **49**, 381 (2006).